European Journal of Pharmaceutics and Biopharmaceutics 169 (2021) 156–167

Contents lists available at ScienceDirect

European Journal of Pharmaceutics and Biopharmaceutics

journal homepage: www.elsevier.com/locate/ejpb

Physiological properties, composition and structural profiling of porcine gastrointestinal mucus

Vicky Barmpatsalou [a], Ilse R. Dubbelboer [a], Agnes Rodler [a,b], Magdalena Jacobson [c], Eva Karlsson [d], Betty Lomstein Pedersen [e], Christel A.S. Bergström [a,*]

[a] The Swedish Drug Delivery Center, Department of Pharmacy, Uppsala University, BMC P.O. Box 580, SE-751 23, Uppsala, Sweden
[b] The Swedish Drug Delivery Center, Department of Medicinal Chemistry, Uppsala University, BMC P.O. Box 574, SE-751 23, Uppsala, Sweden
[c] Department of Clinical Sciences, Faculty of Veterinary Medicine and Animal Sciences, Swedish University of Agricultural Sciences, P.O. Box 7054, SE-750 07, Uppsala, Sweden
[d] Oral Product Development, Pharmaceutical Technology & Development Operations, AstraZeneca, Gothenburg, Sweden
[e] Product Development & Drug Delivery, Global Pharmaceutical R&D, Ferring Pharmaceuticals A/S, Kay Fiskers Plads 11, DK-2300, Copenhagen, Denmark

ARTICLE INFO

Keywords:
Porcine
Gastrointestinal
Mucus
Composition
Structure
Proteomics
Lipidomics
Rheology
Cryo-SEM

ABSTRACT

The gastrointestinal mucus is a hydrogel that lines the luminal side of the gastrointestinal epithelium, offering barrier protection from pathogens and lubrication of the intraluminal contents. These barrier properties likewise affect nutrients and drugs that need to penetrate the mucus to reach the epithelium prior to absorption.

In order to assess the potential impact of the mucus on drug absorption, we need information about the nature of the gastrointestinal mucus. Today, most of the relevant available literature is mainly derived from rodent studies. In this work, we used a larger animal species, the pig model, to characterize the mucus throughout the length of the gastrointestinal tract. This is the first report of the physiological properties (physical appearance, pH and water content), composition (protein, lipid and metabolite content) and structural profiling (rheology and gel network) of the porcine gastrointestinal mucus.

These findings allow for direct comparisons between the characteristics of mucus from various segments and can be further utilized to improve our understanding of the role of the mucus on region dependent drug absorption. Additionally, the present work is expected to contribute to the assessment of the porcine model as a preclinical species in the drug development process.

1. Introduction

The gastrointestinal (GI) mucus is a hydrogel lining the luminal side of the epithelium, throughout the length of the gastrointestinal tract (GIT) [1]. Mucus has a relatively high water content (83–86%) [2]. It creates a pH gradient between the lumen and the epithelium that provides a near neutral environment. It also creates a barrier [3–4] that protects the sensitive epithelial cells from noxious intraluminal contents. In addition, it lubricates the luminal contents by facilitating their propulsion to the lower GIT [5].

From a drug delivery perspective though, the mucus may be viewed as a barrier to absorption [6], as xenobiotics have to permeate through the mucus in order to reach the epithelium, where they can be absorbed. Physiological properties of the mucus, such as pH and water content, determine the ionization state and dissolution potential of drugs close to the epithelium and thus define the microenvironment that permeating drugs encounter prior to absorption. Mucus components such as lipids or the glycosylated regions of mucins may also play a key role in drug diffusion as they might exhibit physicochemical interactions with permeating molecules [6]. Additionally, the barrier function of the mucus—that keeps the bacteria and other pathogens at a safe distance from the GIT epithelium [7]—may pose steric limitations to the diffusing drugs [8]. Thus, to understand the impact of the mucus on drug absorption, the mucus characteristics need to be elucidated.

Early studies on mucus characterization involved mainly rats and mice [1,3], as they are common laboratory animals. Although these studies were fundamental in establishing knowledge about the mucus, the GIT physiology of rodents may not adequately reflect human GIT characteristics, given the GIT differences between rodents and humans [9]. Lower intestinal pH, more water per kg body weight and continuous

* Corresponding author at: Department of Pharmacy, Uppsala University, P.O. Box 580, SE-751 23 Uppsala, Sweden.
E-mail address: Christel.Bergstrom@farmaci.uu.se (C.A.S. Bergström).

https://doi.org/10.1016/j.ejpb.2021.10.008
Received 20 July 2021; Received in revised form 12 October 2021; Accepted 15 October 2021
Available online 20 October 2021

bile secretion are some of the differences between the GIT characteristics of rodents compared to humans [10]. However, accessing GI mucus from healthy volunteers can be ethically challenging and might not yield mucus in appreciative amounts. To address these hurdles, a few studies on GI mucus from larger animal species have been conducted [11–16]. The pig model has gained increased attention from the pharmaceutical industry [17–18] due to the similarities of its GIT to that of humans and its potential for predicting most absorption, distribution, metabolism, excretion and toxicity (ADMET) endpoints [19]. Porcine studies have hitherto focused on the gastric and jejunal mucus. However, drug absorption can be region-dependent [20] and it is therefore essential to obtain information about the nature of the mucus from several GI segments. The present study is the first extensive characterization of mucus from the entire porcine GIT. The aim of this investigation was to elucidate key features (physiological properties, composition and structural profiling) and compare them in the different GIT segments. Our findings provide insights into the nature of the porcine GIT mucus and contribute to the assessment of the potential of the pig as a preclinical species for developing new, orally administered drugs for humans.

2. Materials and methods

2.1. Mucus collection

The GIT of crossbreed Landrace pigs (n = 6), 20–22 weeks of age and 100–110 kg of body weight, was collected from a local abattoir. The animals were slaughtered for commercial meat production and therefore no ethical permit was needed for the purpose of the present study. As per the abattoir's standard routines, the animals were fasted ≥12 h prior to slaughter with water allowed *ad libitum*.

The dissection of the various segments was initiated within 1 h after slaughter and the temperature of the GIT package was monitored throughout the sample collection process. The stomach pouch was dissected and mucus from the stomach was collected. The remaining intestinal tube was cut longitudinally and duodenal mucus was collected 1 cm below the pyloric sphincter. The jejunal and ileal mucus samples were collected from the middle of the small intestine and within 8 cm from the ileocecal valve, respectively. The cecum was dissected and quickly submerged into ice-cold isotonic buffer (10 mM MES buffer containing 1.3 mM $CaCl_2$, 1.0 mM $MgSO_4$ and 137 mM NaCl, pH 6.5) to remove remaining digesta, and after this mucus was collected. Proximal colonic mucus was collected from the first part of the large intestine (distal to the orifice of the cecum) and distal colonic mucus was collected at the beginning of the descendent colon. When necessary, these tissues were also quickly submerged into ice-cold MES buffer, to remove remaining digesta prior to mucus collection. For all tissue segments, the mucus was gently removed using a metallic spatula, to exclude epithelium. Intraluminal contents were also collected from each segment. Both sample types were directly placed on ice to limit bacterial degradation. At least one sample each of mucus and intraluminal contents was collected from each GIT segment of the six pigs, with the exception of one intraluminal duodenum sample which was unavailable. The sample collection was completed within 1 h.

2.2. pH measurements

pH measurements were performed within 1 h after sample collection, using a micro-electrode (Orion Sure-Flow, Thermo Fisher Scientific), after which the samples were aliquoted, snap-frozen in liquid nitrogen, and stored at −80 °C until further analyses.

2.3. Water content determination

Water content was determined based on the weight difference of the samples before and after freeze-drying. Mucus and intraluminal contents were freeze-dried for at least 48 h with a laboratory-scale freeze dryer (VirTis Sentry 2.0, SP Scientific, or a Flexi-Dry MP, FTS systems, both from CiAB, Sweden) with a condenser temperature of −80 °C.

2.4. Proteomics

Label-free and targeted mass tandem (TMT-labelled) global proteomic analyses were performed in the Clinical Proteomics Mass Spectrometry facility (Science for Life Laboratory at Karolinska Institutet/University Hospital). The label-free analysis was performed on mucus samples from the stomach (2 samples: pylorus and fundus), duodenum, jejunum, ileum, cecum, proximal and distal colon from a single pig, while the TMT-labelled analysis was performed on mucus samples from the jejunum (n = 4), proximal (n = 3), and distal colon (n = 3). Data handling was performed using Perseus (version 1.6.14.0) [21], see SI Appendix Text S1. Unique and shared proteins were determined for the label-free analysis using the Venn diagram option in Perseus. When the stomach, small or large intestinal regions are presented, the median of the two (stomach) or three (small and large intestine) mucus samples was used. When a protein was not detected in a mucus sample of that region, that mucus sample was excluded from the calculation. Samples were excluded from the calculation if a given protein was not detected in the GIT segment. Heat maps were created from log2–transformed abundance with Perseus hierarchical clustering using the default settings (Euclidean distance, average linkage and no constraints for the rows and column trees). Significantly higher or lower protein abundance in the jejunal, proximal and distal colonic mucus segments identified with TMT-labelled proteomics were determined with the Volcano plot option in Perseus using the default settings (2-sided *t*-test, with 250 randomizations and a False Discovery Rate (FDR) of 0.05 and S0 of 0.1). Overrepresented classes or pathways and significant differences in the expressed proteins from the TMT-labelled proteome were analyzed on the http://geneontology.org site with the PANTHER overrepresentation test, Reactome version 65 Released 2020-11-17. The data were tested against the *Sus scrofa* reference list, using the Reactome Pathway data sets. The overrepresentation of classes and pathways for all TMT proteins was determined with a Fisher's exact test with a Bonferroni correction. For the significantly differently expressed proteins in the TMT analysis determined with the Volcano plot, the overrepresentation of classes and pathways was determined with a Fisher's exact test with an FDR.

2.5. Lipidomics and metabolomics

Mucus samples of jejunal origin were selected for the lipidomics and metabolomics analyses, as the majority of drug absorption occurs in this segment and for which some literature data was available. Additionally, mucus samples of proximal and distal colonic origin were included in these analyses due to interest in these compartments from sustained release and increased absorption perspectives. This dataset would also allow comparison between mucus from the small and the large intestine. Therefore, mucus samples from the jejunum (n = 2), proximal (n = 3) and distal colon (n = 2) were used for the lipidomics and metabolomics profiling, which was performed at the Swedish Metabolomics Center in Umeå. The lipidomics analysis was performed by LC-MS. Due to the structural heterogeneity of the metabolites present in mucus, both LC-MS and a GC–MS analyses were used for the metabolomics profiling. Further information regarding lipidomics and metabolomics sample work-up and analysis can be found in SI Appendix Text S2 and S3. All lipidomics and metabolomics data were merged into a single file and, when necessary, updated with names, lipid compound classes, Human Metabolome Database ID, and other compound-specific information. Heat maps and Volcano plots of lipid or metabolite abundance were generated with Perseus, using the default settings as described in the section above.

2.6. Rheological characterization

All mucus samples were thawed at room temperature before rheological characterization. The viscoelastic properties of the mucus samples from the upper GIT (stomach, duodenum, jejunum and ileum) were measured using an ARES-G2 strain-controlled rheometer (TA Instruments, Sollentuna, Sweden) with the Advanced Peltier System (APS) accessory for the lower plate. The lower geometry was a 60-mm diameter, APS quick-change flat plate from hardened chromium. A 25-mm stainless steel parallel plate was used as upper geometry. Mucus samples from the proximal and distal colon of all three pigs (P04, P05 and P06) and the mucus sample from the cecum of P05 contained digesta particles in the μm range. In addition, only limited sample volumes (~0.8 ml) were extracted from these segments and therefore the rheological analyses required the use of an 8-mm parallel plate geometry (Discovery Hybrid Rheometer 2 (DHR-2) with the Peltier plate accessory (TA Instruments, Sollentuna, Sweden) using a gap of 500 μm. The two instruments were validated to confirm that they provided comparable data (data not shown).

The apparent viscosity of the mucus samples was measured under continuous flow conditions ramping the shear rate from 0.1 to 100 s^{-1}. The viscoelastic properties of the mucus were calculated from frequency sweeps (Range 0.63–62.8 rad/sec. at 0.3% oscillation strain). The linear viscoelastic region (LVR) was determined for the mucus samples of all segments by performing an amplitude sweep, during which the oscillation strain was increased from 0.1 to 100% at a frequency of 1 Hz oscillation. The 0.3% oscillation strain was within the LVR and thus ensured that sample structure remained intact during the measurements. Measurements were performed in samples from three pigs (P04, P05 and P06). Due to low sample volume from the jejunum of one pig (P05), a jejunal sample from another pig (P03) was used to give triplicate measurements for the jejunum. All measurements were performed at 37 °C (n = 3).

A one-way ANOVA was used to compare differences in the storage modulus (G') values at 1 rad/sec of mucus from the GI segments, followed by Tukey's multiple comparison analysis test; the level of significance was set to 0.05.

2.7. Cryo Scanning Electron Microscopy and Image analysis

The Cryo Scanning Electron Microscopy (CryoSEM) was performed at the Umeå Centre for Electron Microscopy (UCEM). Samples were thawed at room temperature and a single drop from each was casted onto a metal holder, then vitrified in liquid nitrogen. The frozen sample was fractured with a cold knife and sublimated in vacuum at −90 °C for 30 min. Imaging was performed on a Carl Zeiss Merlin field-emission cryogenic scanning electron microscope (cryo-SEM), fitted with a Quorum Technologies PP3000T cryo preparation system. Images were taken at −140 °C using an in-chamber secondary electron detector (ETD) at an accelerating voltage of 2 kV and a probe current of 50 pA. CryoSEM images were appropriately thresholded, converted to binary images, and the pores identified by the ImageJ software (Version 1.52a, NIH, USA). Visual inspection was also carried out to ensure successful pore identification. A minimum of 250 pores were identified from each segment and analyzed for size and shape; the number of replicates (for inter-animal comparisons) was dependent on available mucus volumes and quality of the images obtained. CryoSEM images suitable for image analysis were selected from a single pig for the gastric samples, two pigs for the duodenal, proximal and distal colonic samples, and three pigs for the jejunal, ileal and cecal samples. The pores were characterized in terms of size and shape. Feret's minimum diameter, *i.e.* the shortest distance between any two parallel tangents of a pore, was used as pore size descriptor. The Aspect Ratio (AR), which is defined as the ratio of Feret's max (F_{max}) diameter to Feret's min (F_{min}) diameter (Eq. (1)), was used as the pore shape descriptor.

$$AR = \frac{F_{max}}{F_{min}} \quad (1)$$

2.8. Data Visualization-Statistics

GraphPad Prism (GraphPad Software, CA, USA) was used for data visualization and statistical analyses.

3. Results

3.1. Physiological properties

Visual inspection (under ambient light and with white background) revealed that the mucus and intraluminal samples differed substantially in the various GIT segments (see Fig. 1). The gastric mucus was yellowish and easily visible on the tissue (Fig. 1A and SI Appendix Fig. S1). The small intestinal mucus and intraluminal contents were opaque light orange. The ileal mucus had a pasty consistency, in contrast to the glossy and more fluid mucus from the other small intestinal segments (SI Appendix Fig. S1). Foam was observed in the small intestinal contents and was more pronounced in the jejunal and ileal samples than the duodenal ones (Fig. 1B). All mucus samples of large intestinal origin were translucent gels (SI Appendix Fig. S1). The gastric contents contained remains of undigested straw and other solid food components, whereas only small amounts of feed particles were observed in the small intestinal contents. As expected, the intraluminal contents of the distal colon were more solid than in the upper large intestinal segments (proximal colon and cecum).

The mean mucus pH values and the respective values of the luminal contents are presented in Fig. 1C, D and SI Appendix Fig. S2A. In the stomach, the mean pH of the mucus and the intragastric samples was 5.6, and 4.8, respectively. In the small intestine, the mean duodenal, jejunal and ileal mucus pH values were 6.7, 7.1 and 7.1, respectively. The corresponding values for the respective intraluminal contents were 6.5, 6.9 and 6.8. In the large intestine, the mean cecal, proximal and distal colonic mucus pH values ranged between 7.3 and 7.5. The pH values for the respective intraluminal contents were around 6.8.

The range of the mucus water content was higher and less variable in the stomach (89.0–92.8%) and the large intestinal segments (87.7–94.5%), compared to the small intestinal segments (77.7–91.0%) (Fig. 1E and SI Appendix Fig. S2B). In contrast, the mean water content of the intraluminal contents (87.7–90.9%) was similar for the various gastrointestinal segments, (Fig. 1F), with the exception of distal colon (73.8%). The lower water content was visually confirmed by the solid texture of the distal colonic contents at the time of the collection.

3.2. Proteomics

The label-free analysis revealed that the various regions shared >66% of the proteins *i.e.* they were detected in the stomach, small intestine, and large intestine (Fig. 2A). Excluding the stomach (Fig. 2B and C), the number of shared proteins was over 69% among the intestinal segments, with a low number of unique proteins in these regions (<12% for all segments).

The similarity within each region was also confirmed by the hierarchical clustering (Fig. 2D)—the large intestinal mucus samples formed one cluster, and samples from the small intestinal segment formed another. A comparison of the gastric mucus samples (from the fundus and the pylorus) is found in SI Appendix Text S4 and Fig. S3.

Significant differences in the abundance of proteins in the jejunal, proximal colonic, and distal colonic mucus were identified in the TMT-labelled proteomic data set (Fig. 2E–G, SI Appendix Fig. S4). In the colon, only seven proteins were found to have significantly different abundance in the proximal as compared to the distal colonic mucus. In contrast, over 700 proteins had significantly different levels of

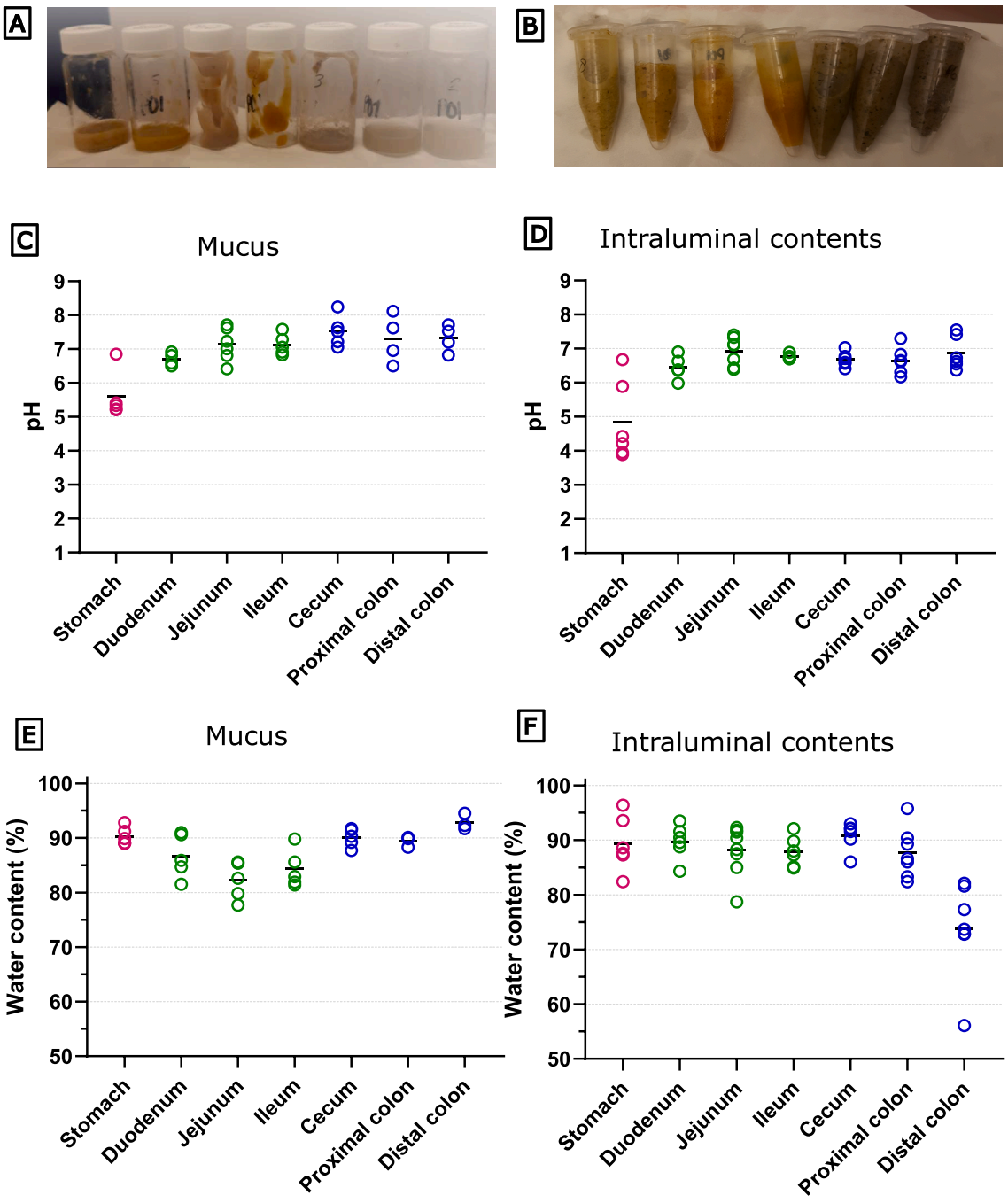

Fig. 1. Physiological properties of porcine gastrointestinal mucus: Visual representation of (left to right) gastric, duodenal, jejunal, ileal, cecal, proximal and distal colonic (A) mucus and (B) intraluminal contents. pH values of (C) mucus and (D) intraluminal contents, water content of (E) mucus and (F) intraluminal contents (% of weight of sample) from various segments of the porcine GIT. Individuals (circles) and mean values (line) are depicted ($n \geq 3$).

abundance in the jejunal mucus than either colonic mucus sample. Among the proteins with higher abundance in the colonic than the jejunal mucus, 235 were significantly more abundant in both proximal and distal colonic mucus. Of the proteins with lower abundance in the colonic mucus than the jejunal, 229 were less abundant in both proximal and distal colonic mucus.

Overrepresentation analysis was performed on the proteins that had significantly higher abundance in colonic or jejunal mucus. This identified several classes which had significantly over-represented numbers of proteins (SI Appendix Fig. S5). In general, mucus from all segments had an overrepresentation of proteins from the metabolism pathways for fructose, lipids, proteins, and amino acids and derivatives. Mucus from the jejunal segment had an overrepresentation of proteins from the digestion and absorption pathways. Mucus from the colonic segments had an overrepresentation of proteins from the O-linked glycosylation of mucins, the immune system, and antimicrobial peptides.

Two gel-forming and four membrane-associated mucins were detected with the label-free analysis (Fig. 2I, J), and one from each group with TMT-labelled analysis (Fig. 2H). The MUC5AC (gel-forming mucin) abundance decreased throughout the intestinal tract, while the MUC2 (gel-forming mucin) abundance remained constant. The hierarchical clustering grouped MUC2 with proteins such as the calcium-activated chloride channel regulator 1 (CLCA1) and IgGFc-binding protein (FCGBP) (SI Appendix Fig. S6). MUC5AC was clustered with carbonic anhydrase 2 and gastrokinine-1, among other proteins.

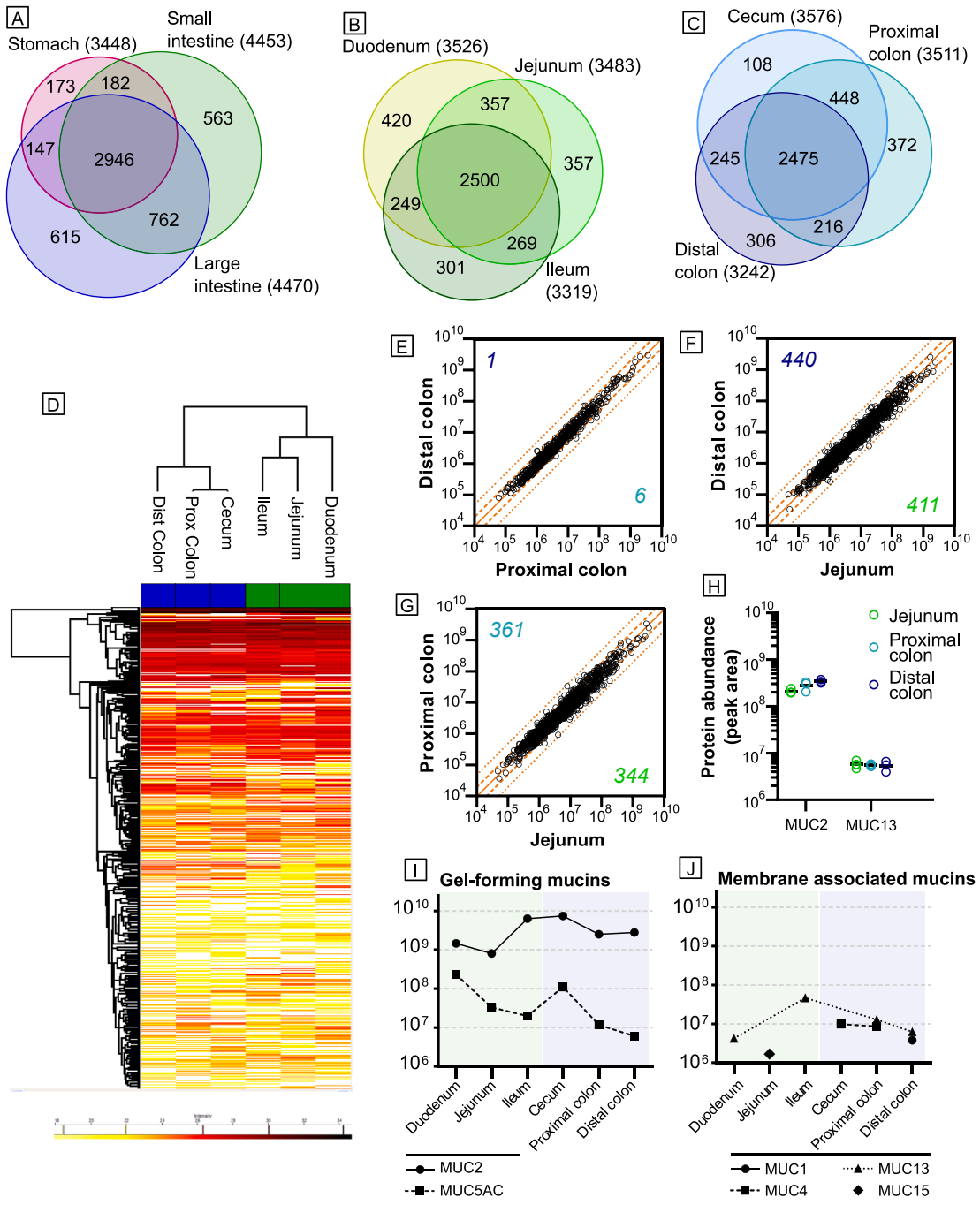

Fig. 2. Composition of porcine gastrointestinal mucus: Combined results of the label-free and TMT-labelled proteomics analyses. The number of shared and exclusive proteins found with global proteomics in GIT regions in Venn diagrams (A); median value of protein abundance was used for the regions. The number of shared and exclusive proteins found with label-free proteomics in the (B) small intestinal and (C) large intestinal regions are shown in Venn diagrams. The numbers in the parentheses correspond to the total number of proteins identified in the various segments. The hierarchical clustering of proteins and mucus samples in the label-free proteomics from the different segments is shown in the heat map (D), with the colour scale bar below in log2 protein abundance. The green and blue squares above the heat map represent the small intestine and large intestine, respectively. (E), (F), and (G) compare protein abundance in the different segments, as measured with TMT-labelled proteomics. The orange solid line represents the line of unity, the dashed lines the 2-fold difference and the dotted lines the 5-fold one. The numbers in these plots represent the number of proteins with significantly higher abundance in the jejunal (green) or colonic (blue) mucus. Mucins detected with TMT-labelled proteomics are presented in (H). Abundance presented for (I) gel-forming mucins and (J) membrane-associated mucins, detected with label-free proteomics in the intestinal segments. (For interpretation of the references to color in this figure legend, the reader is referred to the web version of this article.)

3.3. Lipidomics and metabolomics

LC and GC used for the lipidomics and metabolomics analyses yielded an overlap in detected compounds (SI Appendix Table S1). The largest compound classes were the glycerophospholipids (n = 175), fatty acyls (n = 117), and glycerolipids (n = 78). No significant differences in compound abundance between the proximal and distal colonic mucus were identified (SI Appendix Fig. S7). The colonic mucus samples were therefore considered as one group for the rest of the lipidomics and metabolomics analyses. Most detected compounds (57%) had significantly higher abundance in the jejunal mucus, and only 4% were significantly more abundant in the colonic mucus (Fig. 3, SI Appendix

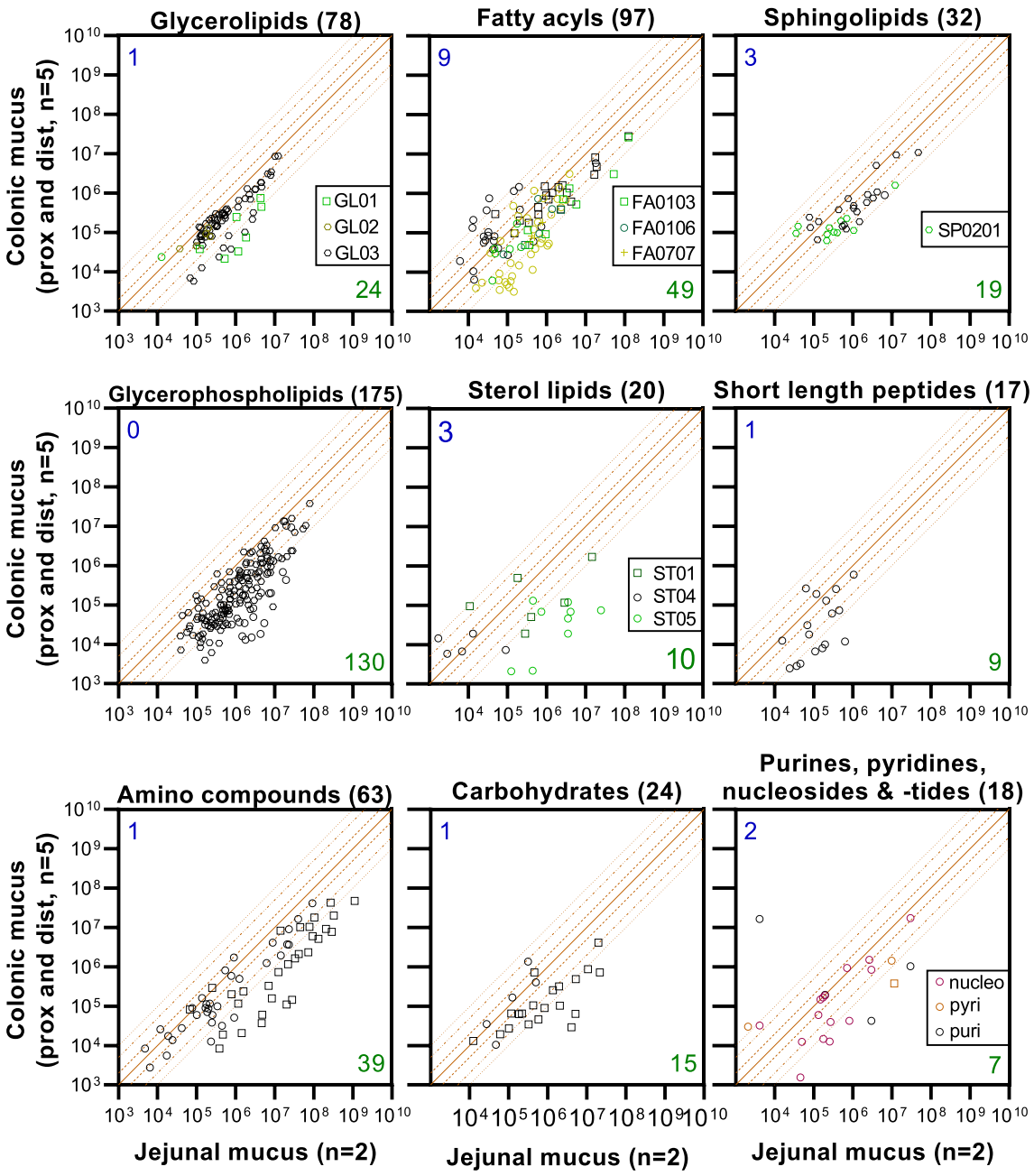

Fig. 3. Composition of porcine gastrointestinal mucus: Correlations of median abundance of lipids and metabolites between the jejunal (n = 2) and combined proximal and distal colonic mucus samples (n = 5). Orange line represents the line of unity (solid), 2-fold (dashed), 5-fold (dashed/dotted) and 10-fold difference (dotted). Values in the plot title represent the number of compounds detected, while the values in the plots represent the number of compounds with significantly higher abundance in the jejunal mucus samples (green) and colonic mucus samples (blue). The compounds were detected with lipidomics (hexagon), metabolomics LC-MS (circle), or metabolomics GC–MS (square). Note that not all detected compounds are shown, and due to different analysis techniques, some compounds might appear twice. See SI Appendix Table S1 for additional information. (For interpretation of the references to color in this figure legend, the reader is referred to the web version of this article.)

Table S1, and Fig. S7). The compound classes in which most of the included compounds had significantly higher abundance in the jejunal mucus were monoradylglycerols (GL01), unsaturated fatty acids (FA0103), hydroxyl fatty acids (FA0106), fatty acyl carnitines (FA0707), sphingoid base 1-phosphates (SP0201), sterols (ST01), and glycine conjugates (ST0503) (Fig. 3). In the glycerophospholipids class (GP), most compounds from all GP subclasses had significantly higher abundance in the jejunal than the colonic mucus, with the exception of monoalkylglycerophosphocholines (GP0106) (SI Appendix Table S1). Of the detected carbohydrates, 63% had significantly higher abundance in the jejunal mucus than the colonic, while only 4% had significantly higher abundance in the colonic mucus.

3.4. Rheological characterization

All mucus samples exhibited viscoelastic properties and non-Newtonian rheological behavior (Fig. 4A–B), with a non-linear relationship between the shear stress and shear rate. The shear-rate dependent rheological profiles of the small intestinal mucus samples are presented in Fig. 4A. Among the small intestinal mucus samples, the ileal ones exhibited the highest mean apparent viscosity values throughout the shear-rate range. These ileal samples were also relatively

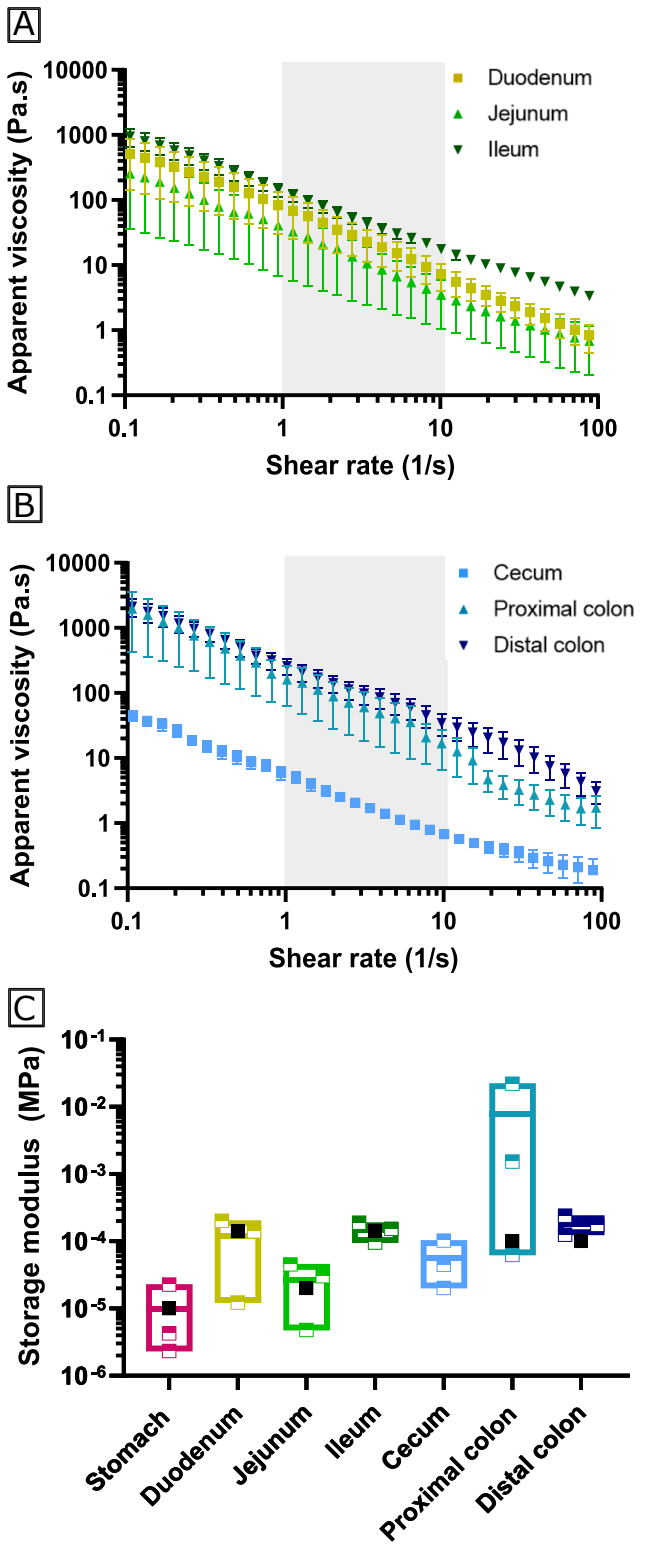

Fig. 4. Structural profiling of porcine gastrointestinal mucus: Apparent viscosity curves of mucus samples from various segments of the porcine (A) small and (B) large intestine as a function of shear rate (mean ± SEM, shaded area illustrates the physiologically relevant shear-rate range [46] (C) Floating bars of storage modulus (G') of mucus samples from the porcine GIT (mean storage modulus value at 1 rad/sec is depicted with line, n = 3). Half-filled squares represent the individual values and black squares the literature values from [45,48–50].

homogenous with limited inter-animal variability (average 2-fold difference between maximum and minimum values). The duodenal samples exhibited lower mean apparent viscosity values than the ileal mucus samples throughout the examined shear-rate range. A 12-fold inter-animal variability was measured for the duodenal mucus. Finally, the jejunal mucus samples exhibited the lowest mean apparent viscosity among the small intestinal ones and the highest inter-animal variability (18-fold difference). The rheological measurements agreed with the visual observations of the jejunal sample texture, which appeared gel-like to liquid-like across animals, resulting in an 18-fold range of apparent viscosity values. The rank order for inter-animal variability was ileum < duodenum < jejunum for the small intestinal mucus samples.

Among the large intestinal mucus samples, the distal colonic mucus samples had the highest mean apparent viscosity values throughout the examined shear-rate range, closely followed by the proximal colonic mucus samples (Fig. 4B). The inter-animal variability of the distal and proximal colonic mucus samples was 4- and 8-fold, respectively. The cecal mucus samples exhibited lower mean apparent viscosity values compared to the distal and proximal colonic ones throughout the examined shear-rate range with a 2-fold inter-animal variability. Hence, the rank order for inter-animal variability was cecum < distal colon < proximal colon for the large intestinal samples.

Under dynamic oscillatory shear conditions, the viscoelastic properties such as storage modulus (G') and loss modulus (G'') were monitored. All mucus samples exhibited predominantly elastic behavior and behaved like true gels, as the storage modulus (G') was higher than the loss modulus (G'') throughout the range of the examined angular frequencies (data not shown). Fig. 4C provides an overview of the storage moduli measured for all mucus segments at 1 rad/sec frequency. Although no statistically significant differences were identified between the mean G′ values (at 1 rad/sec) of the various mucus samples, there was a trend to lower mean storage modulus values in gastric, jejunal and cecal mucus samples, and a trend to higher mean storage modulus values in proximal colonic, distal colonic, ileal, and duodenal mucus samples, indicating a higher degree of crosslinking.

3.5. Microscopic characterization

Cryo-Scanning Electron Microscopy (Cryo-SEM) images revealed an extensive porous gel network for all mucus samples (Fig. 5A–G).

The gel network of gastric and duodenal mucus origin appeared to contain similarly shaped pores of various sizes. According to the image analysis, pores of gastric mucus origin had a lower mean Feret's diameter (4.0 ± 2.0 μm) compared to those of duodenal origin (5.3 ± 2.9 μm), although the pore shape (gastric mean AR: 1.9) was similar (duodenal mean AR: 1.9 μm) (Fig. 5H, I).

Visually, the micro-architecture of the jejunal and ileal mucus was similar and homogenous, containing primarily pores of small size and near circular shape (Fig. 5C and D). The mean Feret's minimum diameter values were 4.0 ± 1.7 μm and 4.1 ± 2.1 μm (Fig. 5H), and mean AR values were 1.7 and 1.8, (Fig. 5I) for the jejunal and ileal mucus samples, respectively.

CryoSEM images of cecal mucus revealed relatively large and elongated pores, while the mucus network in the proximal and distal colon contained both large elongated pores and islets of smaller circular or near circular pores. The mean Feret's minimum diameter of the pore network showed a decreasing trend from the cecal mucus (5.7 ± 3.7 μm), to proximal colonic (5.6 ± 3.5 μm) and to distal colonic (4.2 ± 2.8 μm) mucus. The pore shape was similar in the proximal and distal colonic mucus (mean AR: 1.9 and 1.9, respectively) and slightly more elongated in the cecal mucus (mean AR: 2.1).

4. Discussion

Early work on mucus from the complete GIT focused on determining the mucus thickness using rat [1,22] and mouse models [23]. Although

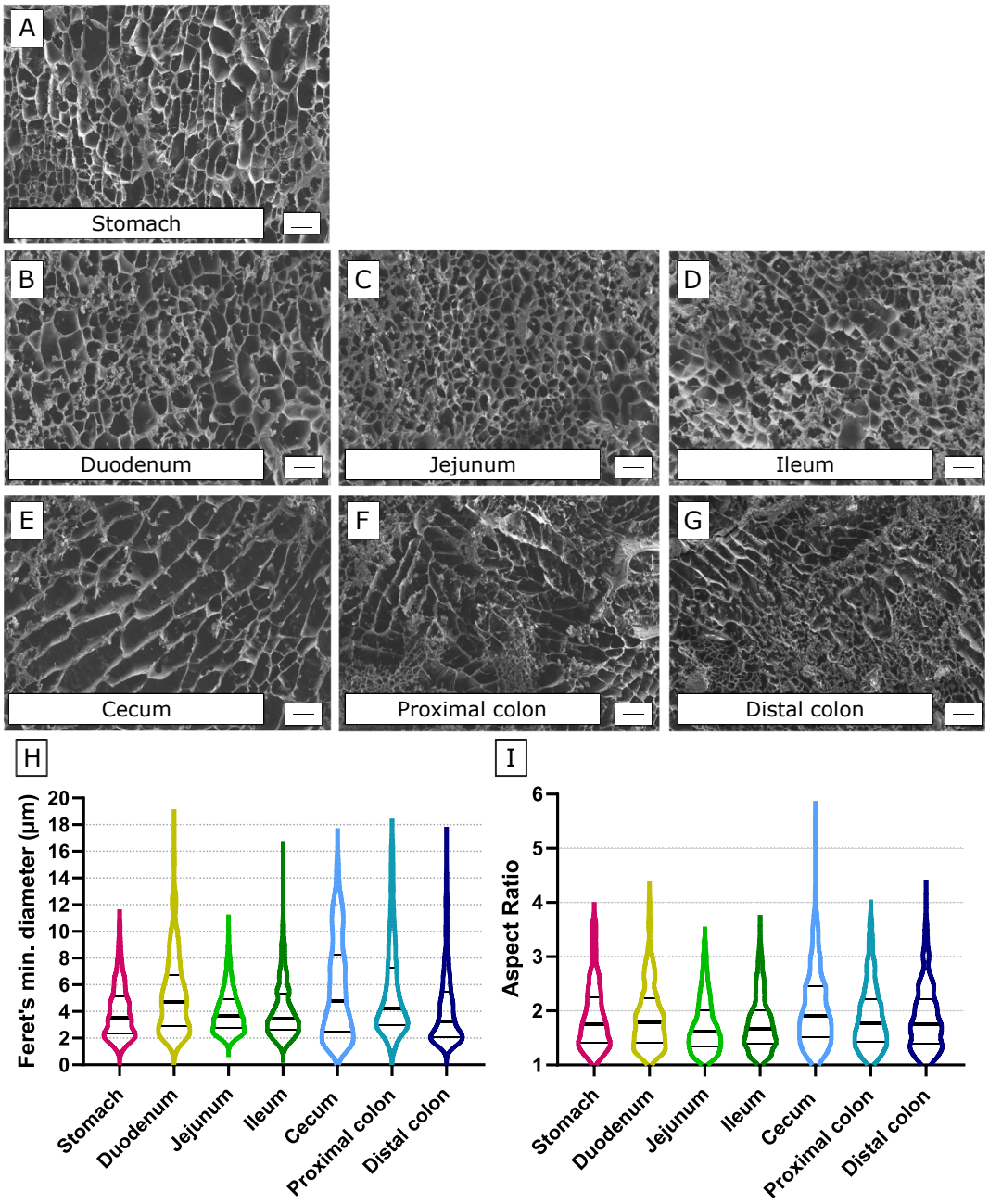

Fig. 5. Structural profiling of porcine gastrointestinal mucus: Representative cryo-scanning electron micrographs of mucus samples collected from (A) stomach, (B) duodenum, (C) jejunum, (D) ileum, (E) cecum, (F) proximal, and (G) distal colon at 2000× magnification. Scale bars: 10 µm. Violin plots of (H) Feret's minimum diameter and (I) aspect ratio distribution—comparison of mucus pores from different segments of the porcine GIT. Light lines represent the 25% and 75% percentiles, while bold line represent the median. At least 250 pores per segment were identified and used in the analysis.

these studies provided fundamental insights into the nature of rodent mucus, nowadays, focus has shifted towards larger animals as preclinical species, given their greater physiological relevance to humans. As such, the pig has been gaining attention as a preclinical species. However, only scarce information is available regarding porcine mucus and this information is mainly based on gastric or jejunal mucus investigations. Therefore, a comprehensive overview that provides insights into the characteristics of mucus from the complete porcine GIT is highly warranted and was addressed in the present study. We report, for the first time, an investigation of the physiological properties, composition, and structural profiling of mucus collected from segments of the entire porcine GIT. The data were compared with literature values where available, and were in good agreement. The present knowledge platform provides a detailed overview of key mucus characteristics that are relevant to drug absorption and allows for comparison among gastrointestinal segments. The findings are also expected to contribute to an improved interpretation of porcine preclinical data given the increasing use of pigs as disease models [24–26].

4.1. Physiological properties

As previously seen in the mouse model, mucus from the various GIT segments differed in appearance and properties [23]. The gastric mucus had a light yellow color, while the small intestinal mucus samples were opaque and had a characteristic orange color, probably due to the presence of bilirubin that is secreted into the bile in the porcine small intestine. The colonic mucus was translucent, as also previously reported [1,27]. Although the pigs were fasted for ≥12 h before slaughter,

there were large quantities of undigested feed and straw in the stomach pouch, suggesting that the pigs had access to bedding straw either shortly before or during transport. This observation is in line with previous studies suggesting that gastric emptying in pigs is bimodal [28], with an initial rapid emptying within the first 15 min and the retention of the gastric contents for up to 24 h. The small intestinal contents were orange, most likely also due to bilirubin. The characteristic foam observed in the small intestinal contents can be attributed to the presence of biological surfactants. Most of the secreted bile acids are reabsorbed in the ileum [29]; therefore, no foam was seen in the large intestinal contents. The water content values of the intraluminal contents were consistent with previous observations [30–32] (SI Appendix Fig. S2F). The high variability in the water content of the gastric contents can be attributed to the *ad libitum* water intake that can vary from animal to animal. As expected, the intraluminal contents progressively condensed into semi-solid material in the distal colon, as the large intestine is a water reclamation site in the pig [31].

4.2. Proteomics

In terms of protein composition, the mucus from each GIT segment was more similar within the same GIT region, compared to mucus from other GIT regions. The protein composition of the gastric mucus samples from the pylorus and the fundus is discussed in SI Appendix Text S4 and SI Appendix Fig. S3.

The various GIT regions are associated with specific functions, and this was reflected in the type of proteins detected in the mucus. Proteins associated with digestion and absorption pathways tended to be overrepresented in jejunal mucus, while antimicrobial peptides and immune system pathways were overrepresented in the colonic mucus. Interestingly, metabolism pathways were overrepresented throughout the GIT mucus. These pathways are related to the metabolism of lipids, proteins, carbohydrates and amino acids, and all of these predominate in the small intestine.

The main site for digestion and metabolism is the small intestine, and the digestive enzymes facilitating these processes are secreted in the stomach (pepsin, which is inactivated in the small intestine and gastric lipase, which remains active) or in the beginning of the small intestine [33]. Therefore, the overrepresentation of metabolism pathways throughout the GIT mucus suggests that mucus from the small intestine—along with the digestive enzymes present therein and intraluminal contents—are transported to lower parts of the GIT via peristalsis.

The presence of the two secreted gel-forming mucins, MUC2 and MUC5AC, is consistent with earlier findings [34]. The predominance of MUC2 in the small and large intestinal mucus has been previously reported in humans [35], pigs [36], mice [37], and rats [38]. The intestinal mucus proteome in humans and mice showed similarities to our hierarchical clustering [35,37] as MUC2, calcium-activated chloride channel regulator 1 (CLCA1), and IgGFc-binding protein (FCGBP) were clustered closely together in these three species. CLCA1 is suggested to be a major component in the mucus and FCGBP is a structural mucus protein. The pig mucus contained galectin-4, while human mucus contains galectin-3, which is a lecithin-binding galactose and part of the core mucus proteome [35].

4.3. Lipidomics – Metabolomics

Most of the lipids and metabolites were significantly more abundant in the jejunal than colonic mucus, which is in line with the physiological function of the porcine small intestine, *i.e.* to digest food and absorb nutrients. The lipid classes and the metabolites, where most compounds had significantly higher abundance, were all digestive products.

Triacylgylcerols are the main type of lipids consumed by non-ruminant animals (GL03) [33]. The digestion of these lipids is initiated by gastric lipase in the stomach and continued by the phospholipases secreted in the pancreatic juice. The triacylglycerols are digested to fatty acids, and mono- and diacylglycerols. Mixed micelles of bile salts, fatty acids, and monoacylglycerols passively transport the digestive products to the cell membrane, where the fatty acids and monoacylglycerols can be absorbed [33]. This would explain the higher availability of these lipids in the jejunal mucus, which was also observed in the present study. The observed glycerophospholipids (GL) and sphingomyelins, can originate from the cell membrane [39], but are also available through the diet, for example from meat, fish, eggs, grains, and soy [39].

However, as the pigs were fasted for 12 h prior to mucus collection, it is more likely that the main source of these lipids were shed-off epithelial cells. The digestion of lipids is achieved by lipases, such as colipase and phospholipases [33], all of which were abundantly found in the proteomic analysis. For most of these enzymes, no significant differences larger than 2-fold between jejunal and colonic mucus abundance were found. Only pancreatic triacylglycerol (PNLIP) had a significantly 5-fold higher abundance in the proximal colonic mucus compared to the jejunal mucus.

In the liver, bile acids are synthesized from cholesterol and further conjugated to glycine (ST0503) or taurine (ST0504) and excreted through the bile to the duodenum [40]. High concentrations of bile salts are maintained throughout the whole small intestine, but they are absorbed in the distal ileum [40]. The present study revealed that all five glycine conjugates and one of four taurine conjugates indeed had significantly higher abundance in jejunal than colonic mucus. Similar numbers of glycine conjugates and taurine conjugates were detected, as reported for guinea pigs [41]. Deconjugation or metabolism of bile salts by bacteria to primary and secondary bile acids occurs in the ileum and colon, by the bile salt hydrolases, 7α-dehydroxylase and 7β-hydroxysteroid dehydrogenase [15,40,42]. Five primary and secondary bile acids were detected and only one had significantly higher abundance in the colonic than jejunal mucus. In the TMT-labelled proteomic analysis, we detected seven hydroxysteroid 17-beta hydrogenases, but no 7α hydroxylase.

The detected metabolites were primarily products that are formed during digestion of proteins and carbohydrates, and were thus more abundant in jejunal than colonic mucus. These were amino compounds, short-length peptides and carbohydrates [43]. Proteolytic enzymes, such as (chymo)trypsin, carboxypeptidases, and other peptidases were found in the proteomics analysis. Carbohydrate digesting enzymes, such as amylases, sucrase, trehalase, lactase and maltase, were also found in the proteomics analysis. The abundance of all proteolytic and carbohydrate digesting enzymes were within a 2.5-fold difference for jejunal and colonic mucus.

4.4. Rheological characterization

All mucus samples proved to be pseudoplastic with shear thinning behavior (the apparent viscosity decreased with increasing shear rate). All mucus samples also posed strong resistance to shear deformation, *i.e.* high apparent viscosity at low shear rates and weak resistance, or low apparent viscosity at high shear rates, see Fig. 4A and B. These data are in agreement with previous assessments of biological gels [44]. The ileal mucus samples exhibited a trend towards slightly higher resistance to flow throughout the physiologically relevant shear rate range (gray area in Fig. 4A), compared to the duodenal and the jejunal mucus. Thus, higher shear stress is required to turn the ileal mucus gel into a low-viscosity fluid that can mix with the luminal contents and eventually be flushed towards the lower parts of the GIT. This observation confirmed visual observations: the ileal mucus samples had a “paste-like” texture, they were too difficult to pipette and required a spatula for handling them. The homogeneity of the ileal samples of all three animals was also reflected in the low inter-animal variability. The mucus of jejunal origin exhibited the lowest resistance to flow and the highest variability among the small intestinal samples. Visually, the texture of jejunal mucus samples ranged from gel-like to liquid-like. Previous data

support the high inter-animal variability for jejunal mucus in pigs [11]. Excessive amounts of mucosal cells in the jejunal mucus compared to colonic mucus have been reported and this observation might be related to the weaker rheological behavior of jejunal mucus [45].

Mucus of proximal and distal colonic origin showed similar resistance to flow, which was higher than the one reported from mucus of small intestinal origin, throughout the physiologically relevant shear rate range [46](Illustrated as gray area in Fig. 4A and B). The higher resistance of large intestinal mucus to flow can be attributed to the presence of the inner mucus layer. This layer forms a tight barrier to protect the epithelium from bacteria in the large intestine; an important property of the hydrogel is to resist shear stress and stay adhered to the epithelium instead of being flushed along with the feces. The cecum is a major fermentation site and is considered part of the large intestine in pigs. However, previous histological work has shown differences in the mucosal architecture between the porcine cecum and colon [47]. These might be related to the substantial differences in the rheological profiles (see Fig. 4B). It is also worth mentioning that the cecum in pigs is a blind sac, and thus the generation of high shear stress forces is limited. All large intestinal mucus samples exhibited lower inter-animal variability than small intestinal samples, again pointing towards the critical need for a shear-resistant hydrogel to exert its important protective role.

The mean storage moduli of the various GIT segments (Fig. 4C) are in accordance with the available literature values for the same species [45,48–50]. There was one exceptionally high storage modulus value from the proximal colon of one pig and this could not be attributed to significant differences of this sample in terms of water content, serum albumin abundance, MUC2 abundance, or pH compared to the other two pig samples. As previously reported, mucus samples of various porcine GIT segments are expected to exhibit similar rheological profiles [12]. In the present study, no statistically significant differences were found among the mean storage modulus values of mucus from various GIT segments. However, variations could be observed, indicating differences in the extent of cross-linking and gel rigidity. This suggests that although the mucins play a key role in the rheological profile of the mucus [51], additional components, e.g., other proteins and lipids, contribute to the viscoelastic properties of the mucus, as previously suggested [36].

4.5. Microscopic characterization

All mucus CryoSEM images collected from the GIT segments showed a highly complex network that cannot be adequately captured with conventional microscopy. The MUC2 mucins, which form the network structure, are highly glycosylated proteins and their individual structure has been extensively studied [52]. Due to their structure, the MUC2 proteins form disulfide bonds between non-glycosylated regions and multiple non-covalent bonds to create the highly entangled network that characterizes the mucus gel [53]. This was observed for all mucus samples in the present study. There have been several studies employing microscopy techniques to determine the pore size of the GIT mucus, reporting values ranging from 20 nm to 200 nm [5,54]. However, particle tracking studies have shown that particles up to 2 μm are able to diffuse through the mucus network [14,23]. This might be because the MUC2 mucins form trimers and they organize as sheets, forming a two-dimensional lamellae network. It has been suggested that these MUC2 mucin networks might contain channels between the lamellae, allowing for diffusion of particles larger than the reported pore size values [54]. The determination of an absolute cut-off value for pore size could be further complicated if one takes into account potential physicochemical interactions between the diffusing molecules and the mucin network. In addition, physiological factors such as secretion of antimicrobial agents from the epithelium (in combination with the size exclusion) might hinder the diffusion of bacteria [55] but not other particles. Therefore, we did not set out to report an absolute cut-off value of the pore size. Rather, we aimed to compare the microarchitecture of mucus and network characteristics from various porcine GIT segments.

CryoSEM revealed similar pore patterns for the gastric and duodenal mucus, which can be explained by the anatomical proximity of these segments. In the distal parts of the small intestine the pore network gradually appears denser and contains mainly small pores of near circular shape. The mucus in the jejunum and ileum had similar networks. The similarity is also confirmed by a study that observed no considerable differences in the porcine jejunal and ileal mucus, neither microscopically nor by multiple particle tracking analysis [16]. In the large intestine, the mucus microarchitecture is considerably more heterogeneous and the presence of large, elongated pores is evident, especially in the cecum. The mucus network of proximal and distal colonic origin consisted of both large elongated pores and smaller ones. This might be related to the presence of two layers in the colon, where the loose layer is formed by proteolytic activity on the inner layer [7]. There is no clear border between the two layers and remains of the outer loose layer may have been collected along with the inner layer.

The large pore size values reported for the colonic mucus samples may be counterintuitive, given the importance of the mucus as a barrier to bacterial diffusion. As previously mentioned, the colonic mucus samples were highly heterogeneous, containing both small and large pores that we hypothesize derive from the presence of the two mucus layers. As bacteria have been reported to penetrate the outer, but not the inner, layer [7], we speculate that this sieve function of the mucus derives most likely from the presence of the small pores. However, other mucus components that are found exclusively in the colonic mucus, e.g., Zg16, which is related with bacteria aggregation activity [56], may play a key role in maintaining a safe distance between the bacteria biomass and the colonic epithelium. Therefore, the regulation of diffusion through the colonic mucus is an interplay between both mucus structural properties and mucus components.

No correlation could be established between Feret's minimum diameter and MUC2, albumin, or total protein content. This suggests that the mucus microarchitecture is co-regulated by other factors, as previously reported [36]. Additionally, the shapes of jejunal and ileal pores are similar to each other and relatively different compared to pores in the gastric, duodenal, proximal and distal colonic mucus. A higher percentage of elongated pores was identified in the cecum than any other segments. These pores of cecal mucus were considerably different in shape from the others. These data suggest that, although MUC2 was the main mucin in all segments except from the stomach (MUC5AC), the final pore network microarchitecture depends on factors other than the mucin type.

5. Conclusion

Our characterization of porcine mucus from various GIT segments provides the first-ever overview of key mucus features and their critical differences.

Mucus from the porcine small and large intestines differ in appearance and water content. Although the protein composition was largely conserved along the GIT, we identified significantly more proteins related to digestive processes in the small intestinal mucus and significantly more related to the immune-response in the large intestinal mucus. The majority of lipids and metabolites were more prevalent in mucus of small intestinal than large intestinal origin. In terms of structural profiling, mucus of small intestinal origin was less viscous and its network composed of smaller, more circular pores, compared to mucus of large intestinal origin.

This work improves our understanding of the key characteristics of the GI mucus that are relevant to drug absorption and can be considered as a step forward towards the evaluation of the porcine model as a valuable preclinical species for oral drug formulation assessment.

Declaration of Competing Interest

The authors declare that they have no known competing financial

interests or personal relationships that could have appeared to influence the work reported in this paper.

Acknowledgments

We are grateful for funding from VINNOVA (2019-00048). The Clinical Proteomics Mass Spectrometry facility at Karolinska Institutet/ University Hospital/ Science for Life Laboratory, is acknowledged for assisting with the proteomics analysis. The Swedish Metabolomics Centre, Umeå, Sweden (www.swedishmetabolomicscentre.se) is acknowledged for metabolic and lipidomic profiling by GCMS and LCMS. The Umeå Centre for Electron Microscopy (UCEM) and the National Microscopy Infrastructure (NMI) are acknowledged for assisting with the CryoSEM analysis.

Appendix A. Supplementary material

Supplementary data to this article can be found online at https://doi.org/10.1016/j.ejpb.2021.10.008.

References

[1] C. Atuma, V. Strugala, A. Allen, L. Holm, The adherent gastrointestinal mucus gel layer: thickness and physical state in vivo, American journal of physiology, Gastrointest. Liver Physiol. 280 (5) (2001) G922–G929.
[2] A.W. Larhed, P. Artursson, E. Björk, The influence of intestinal mucus components on the diffusion of drugs, Pharm. Res. 15 (1998) 66–71.
[3] M. Phillipson, C. Atuma, J. Henriksnäs, L. Holm, The importance of mucus layers and bicarbonate transport in preservation of gastric juxtamucosal pH, American journal of physiology, Gastrointest. Liver Physiol. 282 (2) (2002) G211–G219.
[4] M.E. Johansson, H. Sjövall, G.C. Hansson, The gastrointestinal mucus system in health and disease, Nat. Rev. Gastroenterol. Hepatol. 10 (2013) 352–361.
[5] M. Boegh, C. Foged, A. Müllertz, H. Mørck Nielsen, Mucosal drug delivery: barriers, in vitro models and formulation strategies, J. Drug Delivery Sci. Technol. 23 (4) (2013) 383–391.
[6] P.G. Bhat, D.R. Flanagan, M.D. Donovan, Drug binding to gastric mucus glycoproteins, Int. J. Pharm. 134 (1996) 15–25.
[7] M.E.V. Johansson, M. Phillipson, J. Petersson, A. Velcich, L. Holm, G.C. Hansson, The inner of the two Muc2 mucin-dependent mucus layers in colon is devoid of bacteria, Proc. Natl. Acad. Sci. 105 (2008) 15064–15069.
[8] O. Lieleg, K. Ribbeck, Biological hydrogels as selective diffusion barriers, Trends Cell Biol. 21 (2011) 543–551.
[9] T.T. Kararli, Comparison of the gastrointestinal anatomy, physiology, and biochemistry of humans and commonly used laboratory animals, Biopharm. Drug Dispos. 16 (1995) 351–380.
[10] E.L. McConnell, A.W. Basit, S. Murdan, Measurements of rat and mouse gastrointestinal pH, fluid and lymphoid tissue, and implications for in-vivo experiments, J. Pharm. Pharmacol. 60 (2008) 63–70.
[11] M. Boegh, S.G. Baldursdóttir, A. Müllertz, H.M. Nielsen, Property profiling of biosimilar mucus in a novel mucus-containing in vitro model for assessment of intestinal drug absorption, Eur. J. Pharm. Biopharm.: Off. J. Arbeitsgemeinschaft fur Pharmazeutische Verfahrenstechnik e.V 87 (2) (2014) 227–235.
[12] L.A. Sellers, A. Allen, E.R. Morris, S.B. Ross-Murphy, Mechanical characterization and properties of gastrointestinal mucus gel, Biorheology 24 (6) (1987) 615–623.
[13] L.A. Sellers, A. Allen, E.R. Morris, S.B. Ross-Murphy, Mucus glycoprotein gels. Role of glycoprotein polymeric structure and carbohydrate side-chains in gel-formation, Carbohydr. Res. 178 (1) (1988) 93–110.
[14] A. Macierzanka, N.M. Rigby, A.P. Corfield, N. Wellner, F. Böttger, E.N.C. Mills, A. R. Mackie, Adsorption of bile salts to particles allows penetration of intestinal mucus, Soft Matter 7 (18) (2011) 8077.
[15] A. Macierzanka, A.R. Mackie, L. Krupa, Permeability of the small intestinal mucus for physiologically relevant studies: Impact of mucus location and ex vivo treatment, Sci. Rep. 9 (2019) 17516.
[16] L. Krupa, B. Bajka, R. Staroń, D. Dupont, H. Singh, K. Gutkowski, A. Macierzanka, Comparing the permeability of human and porcine small intestinal mucus for particle transport studies, Sci. Rep. 10 (2020) 20290.
[17] G. Bode, P. Clausing, F. Gervais, J. Loegsted, J. Luft, V. Nogues, J. Sims, The utility of the minipig as an animal model in regulatory toxicology, J. Pharmacol. Toxicol. Methods 62 (2010) 196–220.
[18] C. Colleton, D. Brewster, A. Chester, D.O. Clarke, P. Heining, A. Olaharski, M. Graziano, The Use of Minipigs for Preclinical Safety Assessment by the Pharmaceutical Industry: Results of an IQ DruSafe Minipig Survey, Toxicol. Pathol. 44 (3) (2016) 458–466.
[19] J.W. van der Laan, J. Brightwell, P. McAnulty, J. Ratky, C. Stark, Regulatory acceptability of the minipig in the development of pharmaceuticals, chemicals and other products, J. Pharmacol. Toxicol. Methods 62 (2010) 184–195.
[20] Y. Aoki, M. Morishita, K. Asai, B. Akikusa, S. Hosoda, K. Takayama, Region-Dependent Role of the Mucous/Glycocalyx Layers in Insulin Permeation Across Rat Small Intestinal Membrane, Pharm. Res. 22 (2005) 1854–1862.
[21] S. Tyanova, T. Temu, P. Sinitcyn, A. Carlson, M.Y. Hein, T. Geiger, M. Mann, J. Cox, The Perseus computational platform for comprehensive analysis of (prote) omics data, Nat. Methods 13 (2016) 731–740.
[22] L. Holm, M. Phillipson, Assessment of mucus thickness and production in situ, Methods Mol. Biol. (Clifton N.J.) 842 (2012) 217–227.
[23] A. Ermund, A. Schütte, M.E.V. Johansson, J.K. Gustafsson, G.C. Hansson, Studies of mucus in mouse stomach, small intestine, and colon. I. Gastrointestinal mucus layers have different properties depending on location as well as over the Peyer's patches, Am. J. Physiol.-Gastrointest. Liver Physiol. 305 (5) (2013) G341–G347.
[24] F. Meurens, A. Summerfield, H. Nauwynck, L. Saif, V. Gerdts, The pig: a model for human infectious diseases, Trends Microbiol. 20 (2012) 50–57.
[25] A. Summerfield, F. Meurens, M.E. Ricklin, The immunology of the porcine skin and its value as a model for human skin, Mol. Immunol. 66 (2015) 14–21.
[26] C.S. Rogers, W.M. Abraham, K.A. Brogden, J.F. Engelhardt, J.T. Fisher, J. Paul, B. McCray, G. McLennan, D.K. Meyerholz, E. Namati, L.S. Ostedgaard, R.S. Prather, J.R. Sabater, D.A. Stoltz, J. Zabner, M.J. Welsh, The porcine lung as a potential model for cystic fibrosis, Am. J. Physiol.-Lung Cell. Mol. Physiol. 295 (2008) L240–L263.
[27] G.C. Hansson, Mucus and mucins in diseases of the intestinal and respiratory tracts, J. Intern. Med. 285 (2019) 479–490.
[28] S.S. Davis, L. Illum, M. Hinchcliffe, Gastrointestinal transit of dosage forms in the pig, J. Pharm. Pharmacol. 53 (2001) 33–39.
[29] D. Burrin, B. Stoll, D. Moore, Digestive physiology of the pig symposium: intestinal bile acid sensing is linked to key endocrine and metabolic signaling pathways, J. Anim. Sci. 91 (2013) 1991–2000.
[30] A.G. Low, I.G. Partridge, I.E. Sambrook, Studies on digestion and absorption in the intestines of growing pigs. 2. Measurements of the flow of dry matter, ash and water, Br. J. Nutrit. 39 (1978) 515–526.
[31] J.F. Hecker, W.L. Grovum, Rates of passage of digesta and water absorption along the larg intestines of sheep, cows and pigs, Austr. J. Biol. Sci. 28 (1975) 161–167.
[32] A.L. Rainbird, A.G. Low, Effect of various types of dietary fibre on gastric emptying in growing pigs, Br. J. Nutr. 55 (1) (1986) 111–121.
[33] J. Drackley, Lipid metabolism, Farm Anim. Metabol. Nutrit. 1 (2000) 97–119.
[34] A.P. Corfield, The Interaction of the Gut Microbiota with the Mucus Barrier in Health and Disease in Human, Microorganisms 6 (3) (2018) 78.
[35] S. van der Post, K.S. Jabbar, G. Birchenough, L. Arike, N. Akhtar, H. Sjovall, M.E. V. Johansson, G.C. Hansson, Structural weakening of the colonic mucus barrier is an early event in ulcerative colitis pathogenesis, Gut 68 (12) (2019) 2142–2151.
[36] O.W. Meldrum, G.E. Yakubov, M.R. Bonilla, O. Deshmukh, M.A. McGuckin, M. J. Gidley, Mucin gel assembly is controlled by a collective action of non-mucin proteins, disulfide bridges, Ca(2+)-mediated links, and hydrogen bonding, Sci. Rep. 8 (2018) 5802.
[37] A.M. Rodríguez-Piñeiro, J.H. Bergström, A. Ermund, J.K. Gustafsson, A. Schütte, M.E.V. Johansson, G.C. Hansson, Studies of mucus in mouse stomach, small intestine, and colon. II. Gastrointestinal mucus proteome reveals Muc2 and Muc5ac accompanied by a set of core proteins, Am. J. Physiol. Gastrointest. Liver Physiol. 305 (5) (2013) G348–G356.
[38] V.A. Ferretti, A. Segal-Eiras, C.G. Barbeito, M.V. Croce, Temporal and spatial expression of Muc2 and Muc5ac mucins during rat respiratory and digestive tracts development, Res. Vet. Sci. 104 (2016) 136–145.
[39] P. Castro-Gómez, A. Garcia-Serrano, F. Visioli, J. Fontecha, Relevance of dietary glycerophospholipids and sphingolipids to human health, Prostaglandins Leukot. Essent. Fatty Acids 101 (2015) 41–51.
[40] J.M. Ridlon, D.J. Kang, P.B. Hylemon, Bile salt biotransformations by human intestinal bacteria, J. Lipid Res. 47 (2006) 241–259.
[41] A. Cantafora, D. Alvaro, A.F. Attili, A. Di Biase, M. Anza, A. Mantovani, M. Angelico, Hepatic 3 alpha-dehydrogenation and 7 alpha-hydroxylation of deoxycholic acid in the guinea-pig, Comparat. Biochem. Physiol. B, Comparat. Biochem. 85 (1986) 805–810.
[42] M.H. Foley, S. O'Flaherty, R. Barrangou, C.M. Theriot, Bile salt hydrolases: Gatekeepers of bile acid metabolism and host-microbiome crosstalk in the gastrointestinal tract, PLoS Pathog. 15 (2019), e1007581.
[43] B.E. Goodman, Insights into digestion and absorption of major nutrients in humans, Adv. Physiol. Educ. 34 (2010) 44–53.
[44] R.A. Cone, Barrier properties of mucus, Adv. Drug Deliv. Rev. 61 (2009) 75–85.
[45] L.A. Sellers, A. Allen, E.R. Morris, S.B. Ross-Murphy, The rheology of pig small intestinal and colonic mucus: weakening of gel structure by non-mucin components, Biochimica et Biophysica Acta (BBA) – Gen. Subj. 1115 (2) (1991) 174–179.
[46] A.K. Hardacre, R.G. Lentle, S.-Y. Yap, J.A. Monro, Predicting the viscosity of digesta from the physical characteristics of particle suspensions using existing rheological models, J. R. Soc. Interface 15 (142) (2018) 20180092.
[47] M.S. Hedemann, E. Kristiansen, G. Brunsgaard, Morphology of the large intestine of the pig: Haustra versus taenia, Ann. Anatomy – Anatomischer Anzeiger 184 (4) (2002) 401–403.
[48] B.C. Huck, O. Hartwig, A. Biehl, K. Schwarzkopf, C. Wagner, B. Loretz, X. Murgia, C.M. Lehr, Macro- and Microrheological Properties of Mucus Surrogates in Comparison to Native Intestinal and Pulmonary Mucus, Biomacromolecules 20 (2019) 3504–3512.
[49] H. Bokkasam, M. Ernst, M. Guenther, C. Wagner, U.F. Schaefer, C.M. Lehr, Different macro- and micro-rheological properties of native porcine respiratory and intestinal mucus, Int. J. Pharm. 510 (2016) 164–167.
[50] J. Kocevar-Nared, J. Kristl, J. Smid-Korbar, Comparative rheological investigation of crude gastric mucin and natural gastric mucus, Biomaterials 18 (1997) 677–681.
[51] A.E. Bell, L.A. Sellers, A. Allen, W.J. Cunliffe, E.R. Morris, S.B. Ross-Murphy, Properties of Gastric and Duodenal Mucus: Effect of Proteolysis, Disulfide

Reduction, Bile, Acid, Ethanol, and Hypertonicity on Mucus Gel Structure, Gastroenterology 88 (1) (1985) 269–280.
[52] R. Bansil, B.S. Turner, Mucin structure, aggregation, physiological functions and biomedical applications, Curr. Opin. Colloid Interface Sci. 11 (2-3) (2006) 164–170.
[53] D.J. Thornton, J.K. Sheehan, From mucins to mucus: toward a more coherent understanding of this essential barrier, Proc. Am. Thoracic Soc. 1 (2004) 54–61.
[54] A.N. Round, N.M. Rigby, A. Garcia de la Torre, A. Macierzanka, E.N.C. Mills, A. R. Mackie, Lamellar structures of MUC2-rich mucin: a potential role in governing the barrier and lubricating functions of intestinal mucus, Biomacromolecules 13 (10) (2012) 3253–3261.
[55] F. Xu, J.M. Newby, J.L. Schiller, H.A. Schroeder, T. Wessler, A. Chen, M.G. Forest, S.K. Lai, Modeling Barrier Properties of Intestinal Mucus Reinforced with IgG and Secretory IgA against Motile Bacteria, ACS Infect. Dis. 5 (9) (2019) 1570–1580.
[56] J.H. Bergström, G.M.H. Birchenough, G. Katona, B.O. Schroeder, A. Schütte, A. Ermund, M.E.V. Johansson, G.C. Hansson, Gram-positive bacteria are held at a distance in the colon mucus by the lectin-like protein ZG16, Proc. Natl. Acad. Sci. 113 (2016) 13833–13838.